

# EFFECTS OF ACID HYDROLYSIS TIME ON CELLULOSE NANOCRYSTALS PROPERTIES: NANOINDENTATION AND THERMOGRAVIMETRIC STUDIES

P. KRISHNAMACHARI, R. HASHAIKEH, M. CHIESA and K. R. M. GAD EL RAB

*Materials Science and Engineering Program,  
Masdar Institute of Science and Technology, Abu Dhabi, UAE*

*Received April 27, 2011*

Nanoindentation and thermogravimetric studies were performed on different samples obtained from acid hydrolysis of Microcrystalline Cellulose (MCC). Acid hydrolysis of MCC was carried out using 64% H<sub>2</sub>SO<sub>4</sub> at 45 °C for 10, 20, 30 min, 1 and 5 h, respectively. Elastic modulus and hardness were assessed for each sample. The samples hydrolyzed for 30 min or more had a considerably lower elastic modulus than those hydrolyzed for 20 min or less. Thermogravimetric (TGA) studies revealed that the onset of thermal degradation of all samples occurred at a lower temperature than that of MCC.

**Keywords:** nanocellulose, nanoindentation, acid hydrolysis, thermal analysis

## INTRODUCTION

In recent years, enormous interest has been manifested for producing composite materials with nanosized reinforcement, *i.e.* nanocomposites. This is largely due to the extraordinary properties of these materials, resulting from the nanometric size effect of the reinforcement. The incorporation of these nanosized elements into a polymeric matrix most often results in outstanding properties, as compared to their conventional microcomposite counterparts.<sup>1</sup> Biodegradable polymer nanocomposites have been also extensively studied,<sup>2</sup> with a lot of interest in the fabrication of nanocomposites reinforced by nano-sized cellulosic materials, such as whiskers and fibers isolated from the plant source.<sup>3-4</sup>

Cellulose, the most abundant renewable polymer in the world, is found in plant cell walls, but it can be also synthesized by some bacteria<sup>5</sup> and animals.<sup>6,7</sup> In the presence of strong acids and mechanical forces, native cellulose breaks down into micro- or nano-crystalline cellulose whiskers. Acid hydrolysis of cellulose is a well-known process used to remove amorphous regions and enable isolation of crystallites.<sup>8-11</sup> Disordered or para-crystalline regions of cellulose are preferentially hydrolyzed, whereas the crystalline

regions with higher resistance to the acid attack remain intact. Thus, following an acid treatment that hydrolyzes cellulose (leading to the removal of microfibrils with defects), cellulose rod-like nanocrystals are produced. The preparation and characterization of cellulose nanocrystals has been well-reported in literature.<sup>12-15</sup>

The general characteristic of nanocrystalline cellulose produced through acid hydrolysis depends on conditions such as temperature and time,<sup>16</sup> and on the original source of cellulose fibers: bacterial cellulose,<sup>17</sup> cotton filter paper<sup>18</sup> and tunicates.<sup>19</sup> This huge variety of parameters highlights the need for a screening strategy that can relate the processing conditions to the nanostructure of nanocrystalline materials.

Nanoindentation is a well-established technique that provides powerful means to investigate the mechanical properties of materials at a submicron scale. Since very small volumes are tested, the size effects play an important role and thus nanoindentation shows its potential of being employed in screening of the hydrolysis parameters on the cellulose structure. In the present study, the nanoindentation technique was used to study the modulus and hardness of the prepared samples, starting from the acid

hydrolysis<sup>20</sup> of MCC with 64% H<sub>2</sub>SO<sub>4</sub> for various durations of hydrolysis. Thermogravimetric tests were also performed for all samples, to observe the onset of thermal degradation and to compare it with the nanoindentation behavior. These tests were done to screen the various cellulose samples, with the intention of identifying a suitable candidate, to be used as a reinforcement filler in biodegradable polymers.

### THEORETICAL ANALYSIS OF NANOINDENTATION

Oliver and Pharr<sup>21</sup> utilized the unloading section of the load indentation curve to estimate the reduced modulus of the indented material. The reduced modulus can be evaluated as:

$$E_R = \frac{\sqrt{\pi} \times S}{2 \times \sqrt{A}} \quad (1)$$

where  $S$  is the slope of the unloading force curve evaluated at the maximum indentation depth  $h_{max}$ , as shown in Figure 1. To evaluate the slope, Oliver and Pharr<sup>21</sup> suggested a power law function to fit the unloading force curve:

$$F = a(h - h_r)^m \quad (2)$$

where  $a$  and  $m$  are fitting parameters and  $h_r$  is the residual depth after unloading – as seen in Figure 2. Consequently:

$$S = \frac{dF}{dh} = ma(h - h_r)^{m-1} \quad (3)$$

After evaluating the reduced modulus, the elastic modulus of the indented material can be obtained by knowing the elastic properties of the indenter itself, according to the following formula:

$$\frac{1}{E_R} = \frac{1 - \nu_i^2}{E_i} + \frac{1 - \nu_m^2}{E_m} \quad (4)$$

where  $E_m$ ,  $\nu_m$ ,  $E_i$  and  $\nu_i$  are the elastic modulus and Poisson's ratio for material and indenter, respectively.

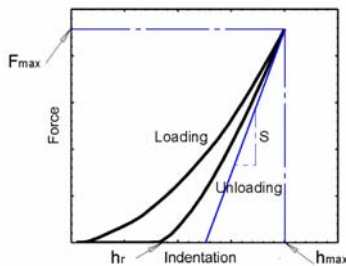


Figure 1: Load indentation curve showing important quantities utilized in nanoindentation analysis

An important input to the reduced modulus equation is the contact area  $A$ , which is a function of tip geometry. The contact area can be evaluated from an area function calibration curve that relates the projected area of the tip with the distance from the tip apex. Such a relationship has to be evaluated prior to analysis. Consequently, the contact area  $A$  is the area function evaluated at contact depth  $h_c$ , as seen in:

$$A = F(h_c) \quad (5)$$

From the elastic surface deformation of the sample under loading, it is observed that the free surface sinks in under the applied load, leading to a contact depth  $h_c$  lower than the maximum depth of indentation  $h_{max}$ , as illustrated in Figure 2:

$$h_c = h_{max} - h_s \quad (6)$$

where  $h_s$  is the elastic sink-in, which can be expressed as:

$$h_s = \varepsilon \frac{F_{max}}{S} \quad (7)$$

where  $\varepsilon = 0.75$ , as suggested by ISO14577. It is worth mentioning that many correction factors have been proposed in literature, to account for some inaccuracies in the obtained results using equation (1), even if there is still no wide agreement on their values or significance.<sup>22-25</sup> Consequently, we have decided to use no correction factors in our analysis. Furthermore, the hardness of the material can be evaluated from the following relation:

$$H = \frac{F_{max}}{A} \quad (8)$$

where  $A$  is again the contact area.

### Calibration of tip area function

Oliver and Pharr<sup>21,24</sup> provided an iterative method to estimate the tip area function of the indenter tip, along with the indenter frame compliance.

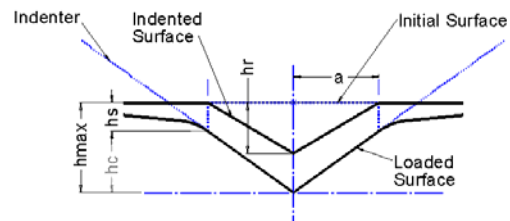


Figure 2: Scheme of material surface deformation during indentation

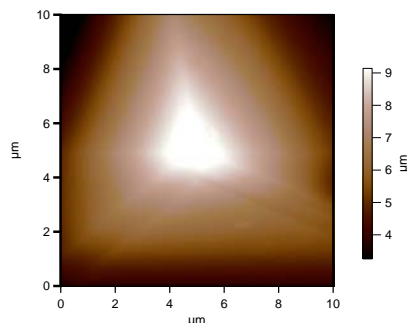


Figure 3: A 10  $\mu\text{m} \times 10 \mu\text{m}$  AFM scan of corner cube tip utilized in the indentation experiment

It has been proven that the method is accurate in a certain indentation range, but the iterative algorithm may converge to a wrong value.<sup>24,26</sup>

In the present work, atomic force microscopy (AFM) has been used to estimate the tip area function. A corner cube indenter tip is scanned on an MFP 3D atomic force microscope (Asylum Research). The scan size is of 10  $\mu\text{m} \times 10 \mu\text{m}$ , for properly describing the overall geometry of the tip. Two major precautions have to be taken into account: thermal drift and AFM tip radius. To minimize thermal drift, the instrument is contained in a thermal acoustic enclosure. Moreover, the AFM tip radius results in the dilation of the indenter tip geometry. To minimize such an effect, a modern sharp tip is utilized (5 nm radius). Figure 3 shows the AFM scan of the indenter tip. After scanning, the tip area function of the corner cube tip is extracted automatically from the AFM software, as seen in Figure 4.

## EXPERIMENTAL

### Sample preparation: acid hydrolysis

Microcrystalline cellulose (Avicell, PH101, Biopolymers) was mixed with 64% sulfuric acid at an initial concentration of 0.1142 g/mL. The mixture was hydrolyzed by stirring at 45 °C. Different batches were made under the same conditions, for durations of 10, 20, 30 min, 1 and 5 h. Hydrolysis was quenched by adding water to the reaction mixture. The 1 h hydrolysis batch was volumetrically split into 2 batches and quenched in water and ethanol, respectively. After quenching, the mixture was allowed to settle overnight in the refrigerator, and the resulting suspension was then centrifuged. Through centrifugation, the hydrolyzed solid cellulose material was separated. The product was then placed inside the dialysis membrane tubes and dialyzed against slow running tap water for 3 days (flow chart in Fig. 5).

About 25 mL of the resulting sample was put in a small beaker and sonicated for 10 min, then subjected to air drying in a shaker (80 °C) for a few hours, until a

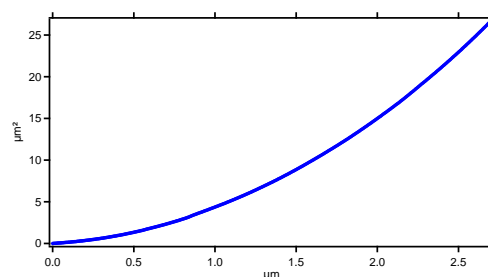


Figure 4: Extracted tip area function for the corner cube tip

dry film was formed. The film was used for obtaining samples for nanoindentation (Fig. 6). For the sake of comparison, a suspension of MCC in water was also tested in the nanoindenter and TGA, by a similar drying procedure.

### Nanoindentation

Nanoindentation measurements were carried out at room temperature with an MFP 3D Asylum Research nanoindenter placed inside an acoustic enclosure. For each run, a series of closely spaced indents were performed within a 20  $\mu\text{m}$  area. The indentation experiment is run in depth control mode. The feedback loop monitors the indentation depth, while the force is recorded correspondingly. This assured a fair comparison between the different cellulose samples.

Series of indentation experiments were performed at varying depths and speeds, before arriving at a testing method of 400 nm depth at 40 nm/s speed. For the sake of comparison, all samples were indented by this method. For every load indentation curve, the elastic modulus and hardness were calculated with the equation mentioned in section 2. The Poisson ratio of cellulose was taken as 0.30. The Poisson ratio and the elastic modulus of the indenter tip (Cube corner tip) were of 0.2 and 865 GPa, respectively.

### Thermal analysis

Thermogravimetric analyses of the various samples were done with a Perkin Elmer (TGA 4000) with a heating rate of 10 °C/min, up to 800°C, in nitrogen environment.

## RESULTS AND DISCUSSION

Nanoindentation experiments permit to determine the hardness and elastic modulus of the indented material. It is interesting to study which quantity is more sensitive to structure variation, as due to the hydrolysis process. The elastic modulus and hardness obtained at a depth of 400 nm measured at 40 nm/s are graphically represented, along with error bars, in Figures 7 and 8, and the numerical values are listed in Table 1.

Figure 7 shows that the elastic modulus of the samples hydrolyzed for 30 min or more is considerably lower than that of the samples hydrolyzed for 20 min or less. However, hardness data show no conclusive pattern. Dong *et al.*<sup>16</sup> found out that longer hydrolysis times generate cellulose rods with larger axial ratios (due to breaking up of the coarse aggregates of cellulose), as well as an increased total surface charge. Larger axial ratios could possibly result in lower interparticle forces, thus causing a decrease in the measured modulus. It is also observed that the 1 h sample did not show much variation in the modulus and hardness values with the two different quenching media (water and ethanol).

It is interesting to investigate the reasons behind the capability of the elastic modulus to detect changes in the cellulose properties. As known, elastic modulus evaluation is directly correlated with the slope of the unloading curve, while the hardness values are directly correlated with the maximum indentation force. Besides, compared to hardness, the elastic modulus is less sensitive to contact area estimation. Figure 9 shows the maximum force measured on the cellulose samples for the same indentation depth. It is obvious that the maximum force values have the same trend of hardness.

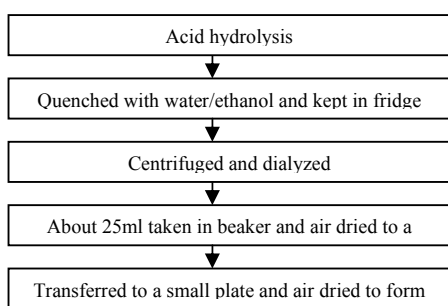


Figure 5: Flow chart of sample preparation technique for nanoindentation



Figure 6: Nanoindentation sample

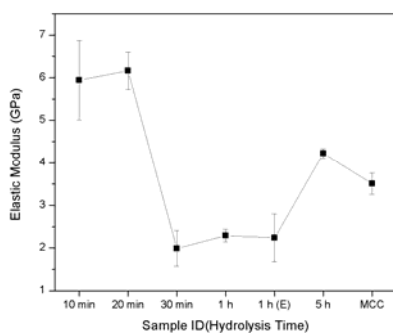


Figure 7: Elastic modulus of various sample IDs with error bars

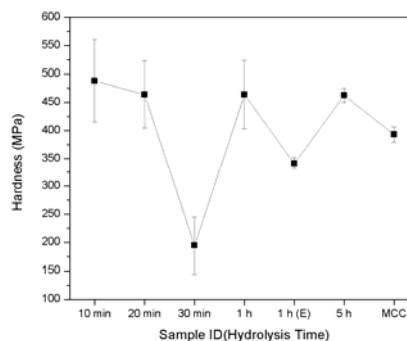


Figure 8: Hardness of various sample IDs with respective error bars

Table 1  
Modulus and hardness values of various hydrolyzed samples (standard deviation is included in the parentheses)

Sample	Modulus (GPa)	Hardness (MPa)
10 min	5.94 (0.93)	488.0 (72.6)
20 min	6.16 (0.44)	463.7 (59.4)
30 min	1.99 (0.42)	194.5 (50.6)
1 h	2.29 (0.15)	463.5 (60.3)
1 h (E)*	2.24 (0.56)	341.4 (10.1)
5 h	4.22 (0.11)	462.4 (12.6)
MCC	3.51 (0.25)	393.1 (13.6)

\*Indicates quenched in ethanol

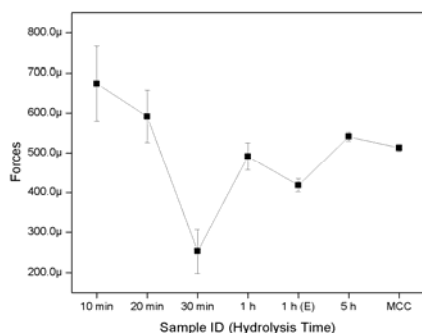


Figure 9: Maximum force values measured for different hydrolysis times. The trend of the force is very similar to that of hardness

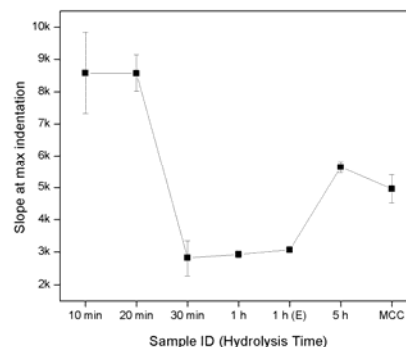


Figure 10: Slope at maximum indentation for different samples. The slope is the main reason for the observation of elastic modulus. Slope measurements can be used as a screening method

The same observation is illustrated in Figure 10 for slope values. It can be inferred that the real parameter for the variation of the mechanical properties of cellulose is the slope of the unloading curves evaluated at maximum indentation depth.

The values of the elastic modulus reported in this experiment are comparable to those obtained by Kunal Das *et al.* (5 to 8 GPa) in their research with hydrolyzed cellulose of varying acid concentrations.<sup>15</sup> However, they are considerably below the values of those reported by researchers who measured the MCC modulus using Raman spectroscopy,<sup>27</sup> and also below the values obtained by molecular mechanics simulation.<sup>28</sup> According to Swadener *et al.*,<sup>29</sup> this discrepancy is due to the fact that the nanoindentation elastic

modulus of an anisotropic material is a mixture of the moduli along all axes, which leads to an underestimation of the higher modulus. The extent of disagreement depends on the degree of anisotropy and on the angle formed between the faces of the indenter body and the load direction.<sup>30</sup> The deformation mechanism of cellulose microfibrils and the extent of stiffness change as a result of this deformation, during an indentation experiment, are unclear. It is worth noting that the loading state of nanoindentation is a collective one, including compressive and shear stresses. This kind of loading provides more realistic properties, which permit to predict the performance of this material in real-life applications.

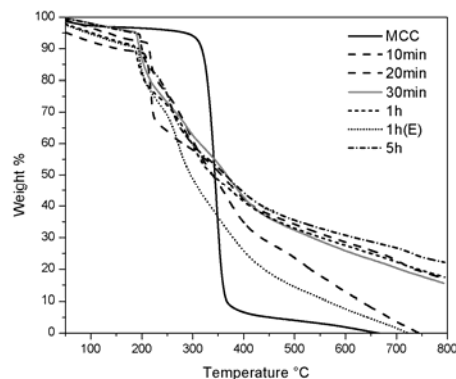


Figure 11: Thermograms depicting mass loss against the temperature of various sample IDs (representing various hydrolysis times)

Thermogravimetric (TGA) studies (Fig. 11), failing as a screening tool, reveal that the onsets

of thermal degradation of all samples occur at a lower temperature than that of MCC, following a

similar pattern. Most of the hydrolyzed samples show residual mass at the end of the heating cycle. The 5 h sample has the highest residual mass at 800 °C. Nanocrystalline cellulose particles show a greater number of free end chains, due to their smaller particle size. The end chains start decomposition at a lower temperature,<sup>31</sup> consequently causing an increase in the char yield of these hydrolyzed samples.<sup>32</sup> Also, the sulfate groups introduced during hydrolysis with sulfuric acid could possibly act as a flame retardant.<sup>33</sup>

## CONCLUSIONS

A facile method for the micromechanical characterization of acid hydrolyzed cellulose has been investigated. Variability of elastic modulus and hardness within samples at various durations of acid hydrolysis of cellulose has been reported. The samples hydrolyzed for 30 min or more have a considerably lower elastic modulus than those hydrolyzed for 20 min or less. The elastic modulus and hardness measured using a nanoindenter may not be absolute values, serving, nevertheless, as a useful screening tool for comparison of such values among various samples. Thermal analysis reveals that most of the hydrolyzed samples show residual mass at the end of the heating cycle. However, the onsets of thermal degradation of all samples occur at a lower temperature than that of MCC. The data here reported will serve as a reference and a selection criterion for acid-treated cellulosic materials that will be used to reinforce biodegradable polymer matrices.

## REFERENCES

- <sup>1</sup> A. Okada *et al.*, *Mater. Res. Symp. Proc.*, **171**, 45 (1990).
- <sup>2</sup> S. Ray and M. Bousmina, *Prog. Mater. Sci.*, **50**, 962 (2005).
- <sup>3</sup> M. A. S. Azizi Samir, F. Alloin and A. Dufresne, *Biomacromolecules*, **6**, 612 (2005).
- <sup>4</sup> M. A. Hubbe *et al.*, *BioResources*, **3**, 929 (2008).
- <sup>5</sup> B. G. Ranby, *Ark. Kemi*, **4**, 249 (1952).
- <sup>6</sup> R. O. Herzog and H. W. Gonell, *Physiol. Chem.*, **141**, 63 (1924).
- <sup>7</sup> B. G. Ranby, *Ark. Kemi*, **4**, 241 (1952).
- <sup>8</sup> S. M. Mukherjee and H. J. Woods, *Biochim. Biophys. Acta*, **10**, 499 (1953).
- <sup>9</sup> R. H. Marchessault, F. F. Morehead and N. M. Walter, *Nature*, **184**, 632 (1959).
- <sup>10</sup> J. F. Revol *et al.*, *Int. J. Biol. Macromol.*, **14**, 170 (1992).
- <sup>11</sup> J. F. Revol *et al.*, *Liq. Cryst.*, **16**, 127 (1994).
- <sup>12</sup> A. Chakraborty, M. Sain and M. Kortschot, *Holzforchung*, **59**, 102 (2005).
- <sup>13</sup> Y. Lu, L. Weng and X. Cao, *Carbohydr. Polym.*, **63**, 198 (2006).
- <sup>14</sup> G. Shlieout, K. Arnold and G. Müller, *AAPS PharmSciTech.*, **3**, 45 (2002).
- <sup>15</sup> K. Das *et al.*, *Cellulose*, **16**, 783 (2009).
- <sup>16</sup> X. M. Dong, J.-F. Revol and D. G. Gray, *Cellulose*, **5**, 19 (1998).
- <sup>17</sup> M. Grunert and W. T. Winter, *Polym. Mater. Sci. Eng.*, **82**, 232 (2000).
- <sup>18</sup> C. D. Edgar and D. G. Gray, *Macromolecules*, **35**, 7400 (2002).
- <sup>19</sup> L. Heux, G. Chauve and C. Bonini, *Langmuir*, **16**, 8210 (2000).
- <sup>20</sup> W. Bai, J. Holbery and K. Li, *Cellulose*, **16**, 455 (2009).
- <sup>21</sup> W. Oliver and G. Pharr, *J. Mater. Res.*, **7**, 1564 (1992).
- <sup>22</sup> T. Chudoba and N. Jennett, *J. Phys., D: Appl. Phys.*, **41**, 215407 (2008).
- <sup>23</sup> M. Troyon and L. Huang, *J. Mater. Res.*, **20**, 610 (2005).
- <sup>24</sup> W. Oliver and G. Pharr, *J. Mater. Res.*, **19**, 3 (2004).
- <sup>25</sup> B. Poon, D. Rittel and G. Ravichandran, *Int. J. Solids Struct.*, **45**, 6018 (2008).
- <sup>26</sup> K. Herrmann *et al.*, *Thin Solid Films*, **377**, 394 (2000).
- <sup>27</sup> S. J. Eichhorn and R. J. Young, *Cellulose*, **8**, 197 (2001).
- <sup>28</sup> F. Tanaka and T. Iwata, *Cellulose*, **13**, 509 (2006).
- <sup>29</sup> J. G. Swadener, R. Jae-Young and G. M. Pharr, *J. Biomed. Mater. Res.*, **57**, 108 (2001).
- <sup>30</sup> W. Gindl and T. Schöberl, *Compos., A: Appl. Sci. Manufact.*, **35**, 1345 (2004).
- <sup>31</sup> J. E. J. Staggs, *Polymer*, **47**, 897 (2006).
- <sup>32</sup> J. Piskorz *et al.*, *J. Anal. Appl. Pyrol.*, **16**, 127 (1989).
- <sup>33</sup> M. Roman and W. T. Winter, *Biomacromolecules*, **5**, 1671 (2004).